Catalysis Today 149 (2010) 334–340

Contents lists available at ScienceDirect

Catalysis Today

journal homepage: www.elsevier.com/locate/cattod

# Assessment of $Fe_2O_3/SiO_2$ catalysts for the continuous treatment of phenol aqueous solutions in a fixed bed reactor

J.A. Botas *, J.A. Melero, F. Martínez, M.I. Pariente

*Department of Environmental and Chemical Technology, ESCET, Rey Juan Carlos University, c/Tulipán s/n, 28933 Móstoles, Madrid, Spain*

ARTICLE INFO

*Article history:*
Available online 30 July 2009

*Keywords:*
Iron catalyst
Mesostructured silica
Phenol
Fixed bed reactor
CWHPO

ABSTRACT

Different iron-containing catalysts have been tested for the oxidation of phenol aqueous solutions in a catalytic fixed bed reactor in the presence of hydrogen peroxide. All the catalysts consist of iron oxide, mainly crystalline hematite particles, over different silica supports (mesostructured SBA-15 silica and non-ordered mesoporous silica). The immobilization of iron species over different silica supports was addressed by direct incorporation of metal during the synthesis or post-synthesis impregnation. The synthesis conditions were tuned up to yield agglomerated catalysts with iron loadings between 10 and 15 wt.%. The influence of the preparation method and the type of silica support was evaluated in a catalytic fixed bed reactor for the continuous oxidation of phenol in terms of catalysts activity (phenol and total organic carbon degradation) as well as their stability (catalyst deactivation by iron leaching). Those catalysts prepared by direct synthesis, either in presence of a structure-directing agent ($Fe_2O_3$/SBA-15(DS)) or in absence ($Fe_2O_3/SiO_2$(DS)), achieved high catalytic performances (TOC reduction of 65% and 52%, respectively) with remarkable low iron leaching in comparison with their silica-based iron counterparts prepared by impregnation. Catalytic results have demonstrated that the synthesis method plays a crucial role in the dispersion and stability of active species and hence resulting in superior catalytic performances.



## 1. Introduction

The degradation of aromatic pollutants such as phenol-like compounds in wastewater streams generated by different industrial activities such as pharmaceutical, petrochemical or chemical industries has emerged as an important concern due to the restrictive environmental laws and regulations. Phenol and phenol-like compounds show high toxicity for microorganisms, high chemical oxygen demand and poor biodegradability [1]. Advanced Oxidation Processes (AOPs) are postulated as interesting alternatives for the destruction of organic pollutants in industrial wastewaters. These processes involve the generation of non-selective and highly reactive hydroxyl radical (•OH), which is one of the most powerful oxidation agents [2], higher than other chemical oxidants commonly used in wastewater treatments.

The use of hydrogen peroxide as an oxidant is an option commercially available for the treatment of industrial wastewaters [3,4]. Nevertheless, the hydrogen peroxide by itself is not effective at high concentrations of refractory compounds due to the fact the reaction rate is very low, even for high oxidant concentrations [5]. In order to promote the generation of hydroxyl radicals and reduce hydrogen peroxide decomposition towards water and oxygen, the use of catalytic processes, such as Fenton systems, could be interesting alternatives. The reaction of hydrogen peroxide with ferrous salts (Fenton's reagent) or other low-valence transition metals (Fenton-like reactions) at room temperature are well known sources of hydroxyl radicals [6,7]. In some cases, temperature has been increased up to 80–120 °C leading to the so-called catalytic wet hydrogen peroxide oxidation (CWHPO) processes. The homogeneous oxidation of organic compounds by means of Fenton-like reactions has been studied in numerous works during last years and it is commercially used to treat industrial wastewaters [8]. However, these homogeneous systems present two main drawbacks. Firstly, the hydroxyl radical production by Fenton-like reactions is strongly dependent on limited pH range (2.5–3.5) and secondly, a final separation of soluble iron species from the treated wastewater is needed.

These drawbacks have promoted the development of Fenton and CWHPO processes based on heterogeneous catalytic systems. Although these processes could show some other disadvantages related with iron leaching, the design of stable and active heterogeneous Fenton-like catalyst has attracted the interest of many researchers. The catalyst design is usually a key factor in order to increase its surface area, minimize the metal sintering, improve its chemical stability and govern the useful lifetime of the catalyst. Therefore, several studies have been addressed to the

* Corresponding author. Tel.: +34 91 488 70 08; fax: +34 91 488 70 68.
*E-mail address:* juanangel.botas@urjc.es (J.A. Botas).

0920-5861/$ – see front matter © 2009 Elsevier B.V. All rights reserved.
doi:10.1016/j.cattod.2009.06.014

incorporation of active iron species over different supports, such as silica, zeolites [9,10], hexagonal mesostructured materials (MCM-41, HMS-9 and SBA-15) [11–15], as well as pillared clays [16] for its application in CWHPO. An interesting overview of solid catalysts has been reported by Perathoner and Centi [17], in which Al–Fe-clays are shown as one group of the most promising catalysts. More recently, the same authors have stated that copper pillared clays are highly effective for CWHPO$_2$ of wastewater streams from olive oil milling production with low loss of copper by leaching [18]. Melero et al. [13] have also reported a remarkable catalytic performance of a novel $Fe_2O_3$/SBA-15 composite catalyst as compared to homogeneous systems as well as a low dependence on the pH for the treatment of phenolic aqueous solutions.

These heterogeneous processes have been carried out in batch operations and phenol is frequently used as a model pollutant. The use of solid catalysts for CWHPO indicates a good perspective of this technology for its application in continuous processes, but it still requires large engineering efforts in modelling and optimal designing of catalyst and industrial reactors. Moreover, their application in continuous systems is normally questioned by the catalyst fouling, in particular for the treatment of wastewater with a complex composition. On the other hand, for its application in fixed bed reactors, catalysts must be shaped into bodies such as granules, spheres and extrudates, in order to decrease the pressure drop and to achieve a convenient mechanical strength. However, there is almost no information in the open literature about its agglomeration process, although this is an essential step regarding its commercial application. Therefore, few works are described in the literature dealing with the treatment of organic pollutants by means of a fixed bed reactor using hydrogen peroxide as oxidant. In this sense, a major experience of continuous processes can be found in catalytic wet air oxidation. In this work, the influence of several silica supports and iron incorporation methods on the degradation of phenol aqueous solutions using a continuous CWHPO process have been assessed.

## 2. Experimental

### 2.1. Preparation of powder and extruded $Fe_2O_3/SiO_2$ materials

Several powder silica-supported iron materials were prepared following two different methods: direct incorporation of the metal during the synthesis and post-synthesis incipient wetness impregnation. In the first strategy, iron was incorporated by direct co-condensation of the silica (TEOS) and iron ($FeCl_3{\cdot}6H_2O$) sources during the synthesis of: (i) mesostructured SBA-15 materials with hexagonal mesoscopic order ($Fe_2O_3$/SBA-15(DS)) following the method described elsewhere [19] and (ii) non-ordered silica support synthesized by means of the sol–gel method, based on acid-catalysed hydrolysis and basic condensation with ammonium hydroxide ($Fe_2O_3/SiO_2$(DS)) [12]. The second method based on the incipient wetness impregnation with $Fe(NO_3)_3{\cdot}9H_2O$ aqueous solution [20] was carried out over: (i) silica SBA-15 material ($Fe_2O_3$/SBA-15(I)), $SiO_2$ sol–gel ($Fe_2O_3/SiO_2$(I)) and commercial silica from PQ Corporation ($Fe_2O_3/SiO_2$-PQ(I)). With the purpose of comparison, a physical mixture of hematite iron oxide ($Fe_2O_3$; Aldrich) with the mesostructured SBA-15 silica ($Fe_2O_3$ + SBA-15(PM)) was also prepared. Prior to the agglomeration of the powder catalysts, all the materials were calcined at 550 °C for 5 h.

$Fe_2O_3/SiO_2$ extrudates were prepared by blending of the powder catalyst with sodium bentonite (see composition in Table 1) (75:25 wt.%) and synthetic methylcellulose polymer (10 wt.% of the previous mixture) which act as binders in the extrusion process [21]. All the components were kneaded with deionised water under high shear conditions until obtaining a homogeneous paste, which was conditioned in a damp atmosphere. Thereafter, the paste was pushed through a ram extruder of 4.8 mm circular die and the resultant rod-shaped materials were dried for 3 days in a climatic chamber under controlled temperature and relative humidity (RH) from 20 °C and 70% RH to 40 °C and 10% RH. Finally, the extrudates were calcined in air until 650 °C (2 h) using a slow ramp of temperature, in order to achieve a gradual removal of water and the organic content and strengthening the mechanical consistence of the material by sintering of the inorganic binder. The final pellets for the catalytic reactions were crushed and sieved until particle sizes with spherical-like shape and an average diameter between 1.6 and 2 mm.

**Table 1**
Bentonite weight composition.

| Components | Chemical composition (wt.%) |
|---|---|
| $SiO_2$ | 55.20 |
| $Al_2O_3$ | 9.74 |
| $Fe_2O_3$ | 4.62 |
| MgO | 22.20 |
| CaO | 2.67 |
| $Na_2O$ | 2.21 |
| $K_2O$ | 2.18 |
| $TiO_2$ | 0.60 |
| $SO_3$ | 0.24 |
| MnO | 0.08 |
| BaO | 0.08 |
| Others | 0.18 |

### 2.2. Catalysts characterization

Physicochemical and textural properties as well as the presence of crystalline phases of the powder materials and extruded catalysts were analyzed by means of different conventional techniques. X-ray powder diffraction (XRD) data were acquired on a Philips X-Pert diffractometer using Cu Kα radiation. The data were collected ranging $2\theta$ from 0.5° to 50° with a resolution of 0.02°. Nitrogen adsorption and desorption isotherms at 77 K were measured using a Micromeritics Tristar 3000 System. Transmission electron microscopy (TEM) images were taken on a Philips Tecnai-20 electron microscope operating at 200 kV. SEM images were obtained in a XL30 ESEM FEI (PHILIPS) electron microscope. The iron content of the synthesized materials was measured by means of Atomic Emission Spectroscopy with Induced Coupled Plasma (ICP-AES) analysis performed in a Varian Vista AX system.

### 2.3. Catalytic tests in an up-flow fixed bed reactor

Fig. 1 depicts the experimental set-up used for the degradation of phenol aqueous solutions by means of catalytic wet hydrogen peroxide oxidation (CWHPO). The tubular reactor was made of glass with inner diameter of 1.2 cm and 15 cm of length. The catalyst particles were packed between glassy beads to enable a better distribution of the inlet solution inside the catalyst bed and achieve the desired temperature. The operating conditions for the evaluation of the activity and stability of the synthesized materials were set according to preliminary studies with this experimental set-up [22]: (i) reactor temperature ($T_R$) of 80 °C, (ii) 1 mL/min of feed flow rate ($Q_A$) and (iii) 2.9 g of catalyst with a particle size between 1.6 and 2 mm. The concentration of reactants in the feed tank was 1 g/L of phenol and 5.1 g/L of $H_2O_2$ (stoichiometric amount for the complete phenol mineralization, according to the reaction (1)). Note that the organic removal in the feed tank along the catalytic assays was almost negligible (TOC conversion lower than 2%). The residence time for the liquid phase was of 3.8 min calculated following the procedure previously described in

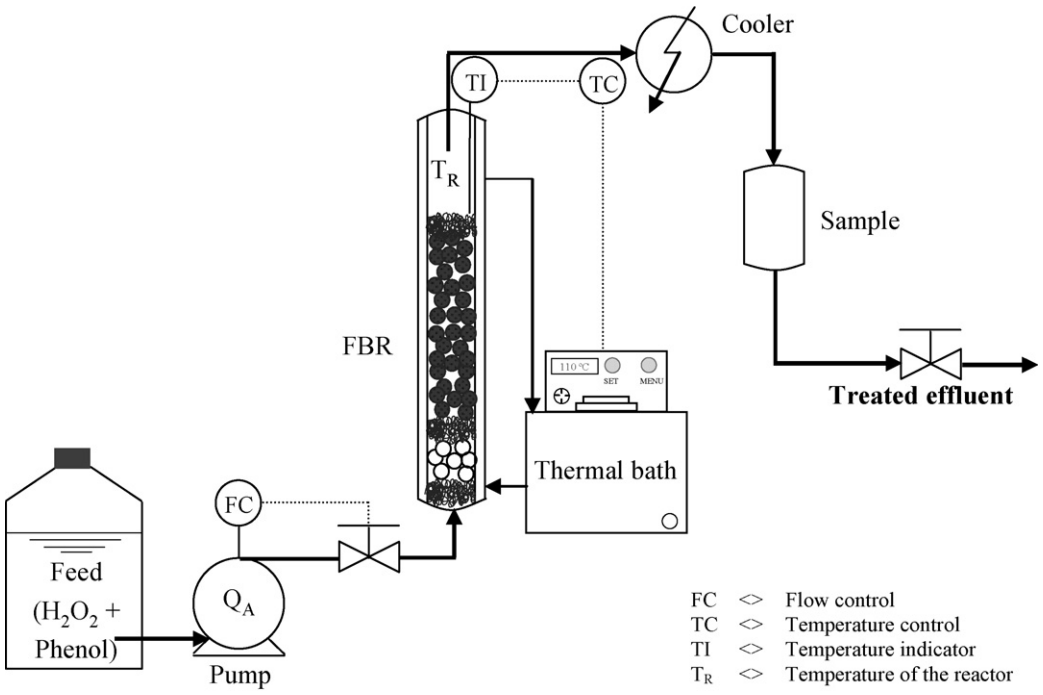


**Fig. 1.** Experimental set-up of the up-flow fixed bed reactor for the catalytic wet hydrogen peroxide oxidation of phenol aqueous solutions.

literature taking into account the bed porosity ($\varepsilon$) and the liquid hold up ($h_L$) of the packed bed [22].

$$C_6H_5OH + 14H_2O_2 \rightarrow 6CO_2 + 17H_2O \quad (1)$$

Samples were hourly withdrawn from the treated effluent to determine Total Organic Carbon (TOC), phenol and hydrogen peroxide concentrations, as well as iron leached out from the catalyst to the treated effluent. TOC content of the solutions was analyzed using a combustion/non-dispersive infrared gas analyser model TOC-V Shimadzu. Phenol conversion was determined by means of HPLC chromatograph (Varian Prostar) equipped with a Waters Spherisorb column and an UV detector adjusted at 215 nm, employing ultrapure water acidified with $H_3PO_4$ up to pH 2.7 as mobile phase. Hydrogen peroxide conversion was determined by iodometric titration. Iron content in the treated solution was measured by inductively coupled plasma-atomic emission spectroscopy (ICP-AES) analysis performed in a Varian VISTA AX system. The performance of the reaction was studied following the TOC conversion ($X_{TOC}$), oxidant consumption ($X_{H_2O_2}$) and oxidant efficiency ($\eta$) as described by Eqs. (2)–(4).

$$X_{TOC}\,(\%) = \frac{[TOC]_{inlet} - [TOC]_{outlet}}{[TOC]_{inlet}} \times 100 \quad (2)$$

$$X_{H_2O_2}\,(\%) = \frac{[H_2O_2]_{inlet} - [H_2O_2]_{outlet}}{[H_2O_2]_{inlet}} \times 100 \quad (3)$$

$$\eta = \frac{\text{theoretical consumption of } H_2O_2}{\text{real consumption of } H_2O_2} \quad (4)$$

The theoretical $H_2O_2$ consumption needed for the removal of obtained TOC conversion can been estimated according to the reaction (5).

$$C + 2H_2O_2 \rightarrow CO_2 + 2H_2O \quad (5)$$

## 3. Results and discussion

### 3.1. Catalysts characterization

Table 2 shows the physicochemical properties of the synthesized powder and extruded iron catalysts, as well as the silica materials used as supports for impregnation. The materials have been classified in different groups depending on the silica support: mesostructured SBA-15, mesoporous silica obtained via sol–gel

**Table 2**
Characterization data of iron-containing catalysts supported over silica materials.

| Material (synthesis method) | Support | Powder | | | Extruded | | |
|---|---|---|---|---|---|---|---|
| | | $S_{BET}$ ($m^2$/g) | Vp ($cm^3$/g) | Fe (wt.%) | $S_{BET}$ ($m^2$/g) | Vp ($cm^3$/g) | Fe (wt.%) |
| SBA-15 | SBA-15 | 790 | 1.21 | – | – | – | – |
| $Fe_2O_3$/SBA-15(I) | | 549 | 0.78 | 15.8 | 333 | 0.53 | 12.4 |
| $Fe_2O_3$/SBA-15(DS) | | 475 | 0.67 | 18.0 | 264 | 0.48 | 14.0 |
| $Fe_2O_3$ + SBA-15(PM) | | – | – | – | 277 | 0.49 | 13.8 |
| $SiO_2$ | $SiO_2$ sol–gel | 296 | 1.79 | – | – | – | – |
| $Fe_2O_3$/$SiO_2$(I) | | 207 | 0.85 | 15.9 | 180 | 0.62 | 12.0 |
| $Fe_2O_3$/$SiO_2$(DS) | | 270 | 0.69 | 14.8 | 225 | 0.55 | 11.1 |
| $SiO_2$-PQ | $SiO_2$ PQ | – | – | – | 346 | 1.16 | – |
| $Fe_2O_3$/$SiO_2$-PQ(I) | | – | – | – | 252 | 0.87 | 15.4 |

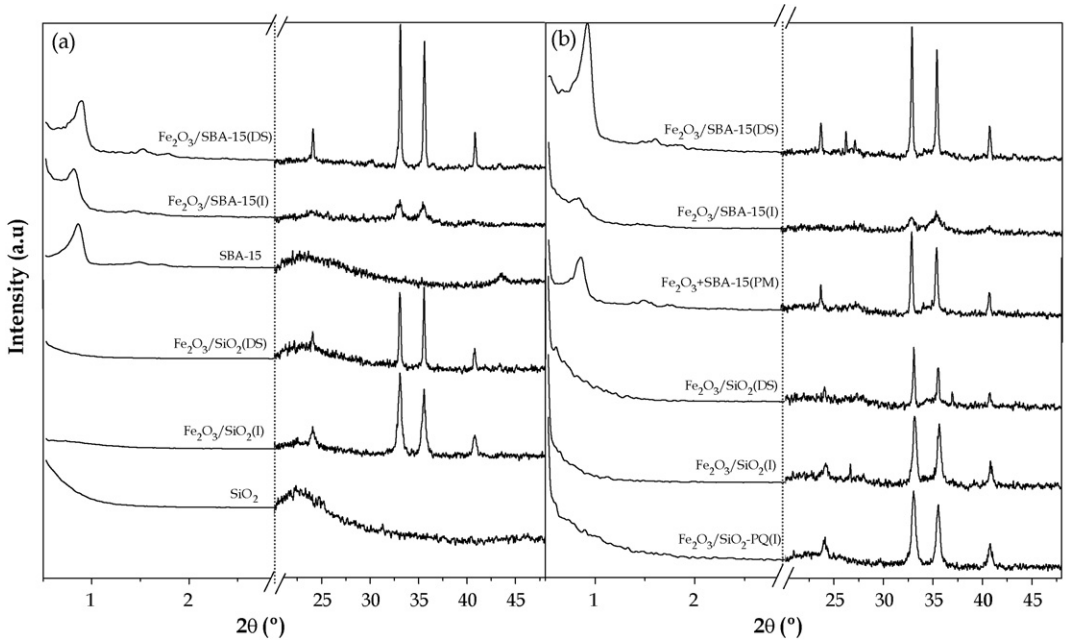


**Fig. 2.** XRD patterns of (a) powder and (b) extruded iron-containing materials over mesostructured SBA-15 and non-ordered mesoporous silica supports.

and commercial extruded mesoporous silica acquired from PQ Corporation. As can be seen, the first group corresponds to hexagonal mesostructured SBA-15 materials, where iron was incorporated by direct synthesis ($Fe_2O_3$/SBA-15(DS)) and incipient wetness impregnation ($Fe_2O_3$/SBA-15(I)). Additionally, a physical mixture of hematite iron oxide and the SBA-15 silica support ($Fe_2O_3$ + SBA-15(PM)) was also prepared. The second group includes mixed $Fe_2O_3/SiO_2$ materials synthesized by simultaneous condensation of iron and silica sources via the sol–gel method ($Fe_2O_3/SiO_2$(DS)) or impregnation of mesoporous silica sol–gel ($Fe_2O_3/SiO_2$(I)). Finally, the third group is constituted by impregnated commercial silica support ($Fe_2O_3/SiO_2$-PQ(I)).

Characterization data of powder materials evidence that catalysts based on SBA-15 silica supports have higher specific surface areas than those supported over the silica synthesized via sol–gel. This is due to the narrow pore size distribution of mesoporous SBA-15 channels (7–9 nm) with hexagonal arrangement, which provides remarkable surface areas and pore volumes (650–800 $m^2$/g and 1–1.2 $cm^3$/g, respectively). In contrast, silica sol–gel materials depict broader pore size distributions and higher average pore diameter than SBA-15 based materials, which lead to higher ratio between pore volume and specific surface area. As a result of the iron incorporation process over both silica supports, a significant reduction of surface area and pore volume were evidenced for all the catalysts, although this fact was particularly more accentuated for the incorporation of iron by direct synthesis over SBA-15 materials ($Fe_2O_3$/SBA-15(DS)) [23]. Nevertheless, the powder catalysts synthesized over SBA-15 supports show higher specific surface areas regardless of the synthesis method (475 and 549 $m^2$/g, for $Fe_2O_3$/SBA-15(DS) and $Fe_2O_3$/SBA-15(I), respectively) than the counterparts supported over non-ordered mesoporous silica (270 and 207 $m^2$/g for $Fe_2O_3/SiO_2$(DS) and $Fe_2O_3/SiO_2$(I), respectively).

XRD patterns illustrated in Fig. 2 evidence typical diffractions of the hexagonal arrangement of mesoporous materials for powder iron-containing SBA-15 catalysts in the low angle range, whereas iron catalyst prepared by sol–gel method or impregnation over silica sol–gel does not show any sign of mesoscopic order. At higher angles, clear diffraction peaks at 33°, 36° and 42° are observed, which are characteristic of crystalline hematite iron oxide particles, except for $Fe_2O_3$/SBA-15(I) catalyst. This fact could be related to the small size of the crystalline iron oxide particles which makes it less visible to the X-ray diffraction. Moreover, iron amorphous phases were not detected in this sample. The comparison between XRD pattern of powder and extruded materials indicates that the characteristic diffractions of hematite iron oxide particles are not affected by the agglomeration process. Additionally, the hexagonal mesoscopic order of SBA-15 materials was also retained.

As can be seen in Table 2, the percentage of iron incorporated over the powder catalysts ranged from 15 to 18 wt.%, whereas for agglomerated materials decreased up to 11–15 wt.%. This reduction is consequence of the dilution effect related to the inorganic bentonite clay incorporated into the extruded material during the agglomeration process. Moreover, the specific surface area of the agglomerated materials significantly decreased in comparison with the powder counterparts. This phenomenon is also attributed to the amount of bentonite clay incorporated in the extruded material, which presents a low surface area (19 $m^2$/g), as well as the sintering process that take place during the final calcination step. Interestingly, the effect of the sintering process seems to be more important in SBA-15-based iron catalysts, which suffer 40–45% of surface area reduction, than iron catalyst supported over non-ordered silica sol–gel materials (with reductions in the range 13–16%). Nevertheless, iron-containing catalysts based on mesostructured SBA-15 silica matrices still exhibit higher specific surface areas. Pore size distribution profiles shown in Fig. 3 for agglomerated catalysts confirm the characteristic pore size distribution of mesostructured SBA-15-type materials with a narrow pore size distribution centred at 8–9 nm, as compared to those shown by non-ordered mesoporous materials prepared by the sol–gel method with a broader pore size distribution. Unlike the physical mixture of $Fe_2O_3$ + SBA-15(PM) which have shown the highest pore diameter (8.8 nm), the iron incorporation over SBA-15 silica support by direct synthesis or impregnation have yielded a slight reduction of the pore diameter up to ca. 7.7 and 8.2 nm, respectively. Regarding to iron catalysts supported over non-ordered mesoporous silica, the sample $Fe_2O_3/SiO_2$(DS) exhibits a broader pore size distribution centred at ca. 15 nm as compared to the other two catalysts of this group.

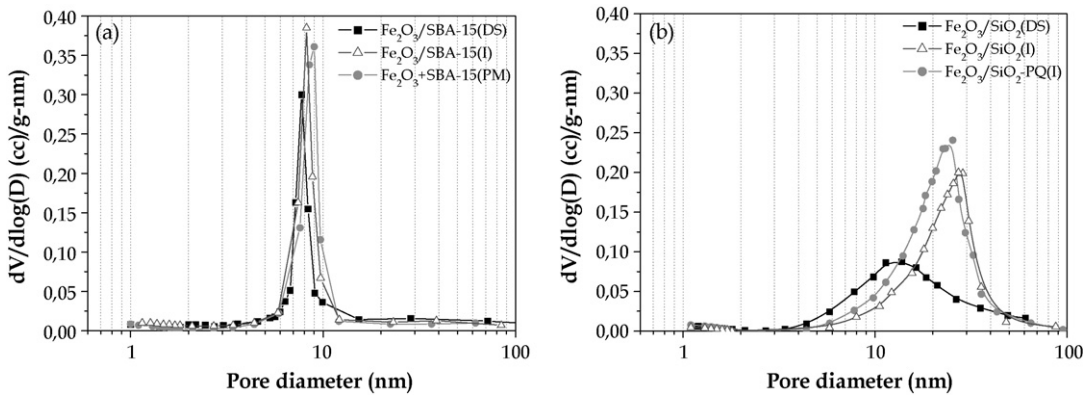


**Fig. 3.** Pore size distribution of the extruded materials: (a) supported over SBA-15 and (b) supported over non-ordered mesoporous $SiO_2$.

TEM images of extruded iron catalysts (Fig. 4) confirm the hexagonal arrangement of SBA-15-based materials. In both groups of iron-containing catalysts, mesostructured SBA-15 and non-ordered mesoporous silica materials, the iron particle size is strongly dependent on the synthesis method and type of silica support. Interestingly, $Fe_2O_3/SiO_2$(DS) catalyst, prepared by the sol–gel method, evidence a remarkable dispersion of iron particles over the $SiO_2$ support. Unlike iron impregnated catalysts over non-ordered mesoporous silica sol–gel ($Fe_2O_3/SiO_2$(I)) and silica-PQ ($Fe_2O_3/SiO_2$-PQ(I)), impregnated $Fe_2O_3$/SBA-15(I) catalyst shows a better dispersion of smaller iron particles over the silica framework. These data seem to be in agreement with the small iron oxide particle sizes assumed from the X-ray diffraction patterns. The presence of agglomerating bentonite layers can be also observed together with the silica support and iron oxide particles.

### 3.2. Catalytic treatment of phenolic aqueous solutions in a fixed bed reactor

The catalytic performance of iron-containing materials for the wet peroxide oxidation of phenol aqueous solutions was evaluated in terms of TOC reduction, phenol degradation and hydrogen peroxide conversion. Likewise, the stability of the catalysts along the treatment was also studied analyzing the iron concentration leached out from the catalyst within the treated outlet effluent.

The feasibility of the iron catalysts for the continuous treatment of a phenol aqueous solution can be demonstrated by the results of TOC and hydrogen peroxide conversion (Fig. 5). TOC conversion profiles revealed different times of stabilizing up to steady-state conditions ranging from 1 to 3 h, except for the physical mixture of $Fe_2O_3$ + SBA-15(PM), which needs almost 7 h. Although this enlargement of the stabilizing time has not been deeply studied, this phenomenon might be related to particular diffusional constraints associated with the accessibility of the supported iron particles depending on the silica support and the type of synthesis method. Nevertheless, it must be remarked the stability of the TOC degradation values once the steady state is reached, with constant values up to 8 h on stream for all the catalysts, excepting $Fe_2O_3$ + SBA-15(PM). Results of TOC evidence a high catalytic performance of SBA-15-based iron catalysts with conversions above 60%. In the case of sol–gel materials, $Fe_2O_3/SiO_2$(I) keep a similar TOC conversion (64%), whereas $Fe_2O_3/SiO_2$(DS) undergoes a slight reduction up to 52%. In contrast, impregnated commercial silica PQ ($Fe_2O_3/SiO_2$-PQ(I)) shows a striking decrease of the TOC degradation until ca. 25%.

Moreover, as it can be seen in Fig. 5c and d, the hydrogen peroxide profiles follow a parallel trend to the TOC conversion and in all the cases, except for the physical mixture, a steady oxidant conversion of 100% is obtained after 2 h on stream (Table 3). Regards the efficient use of the oxidant, the $\eta$ parameter ranges from 0.5 to 0.6 for all the catalyst except $Fe_2O_3/SiO_2$-PQ(I) catalyst

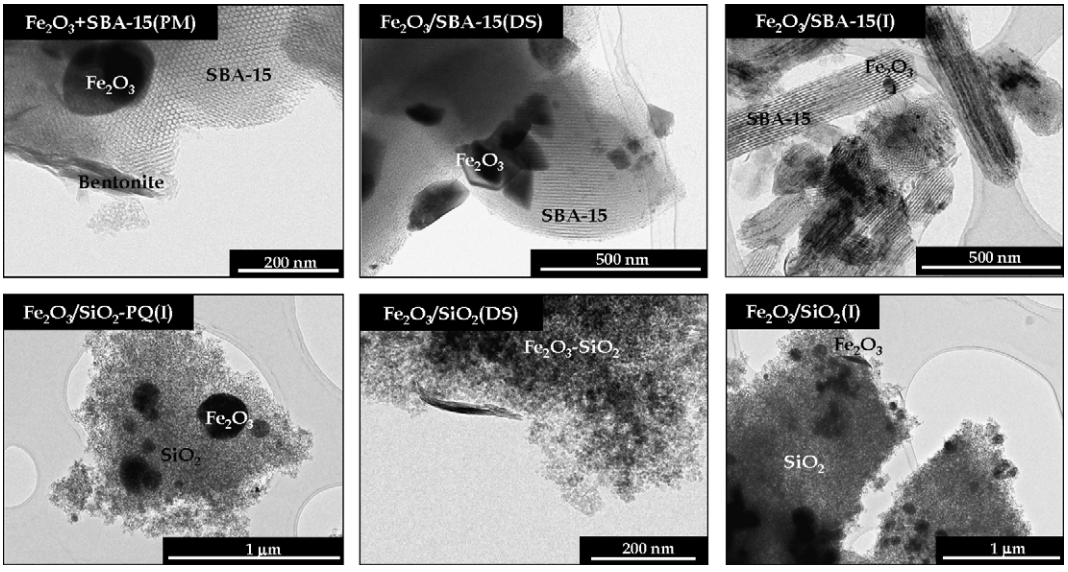


**Fig. 4.** TEM images of the extruded iron-containing materials.

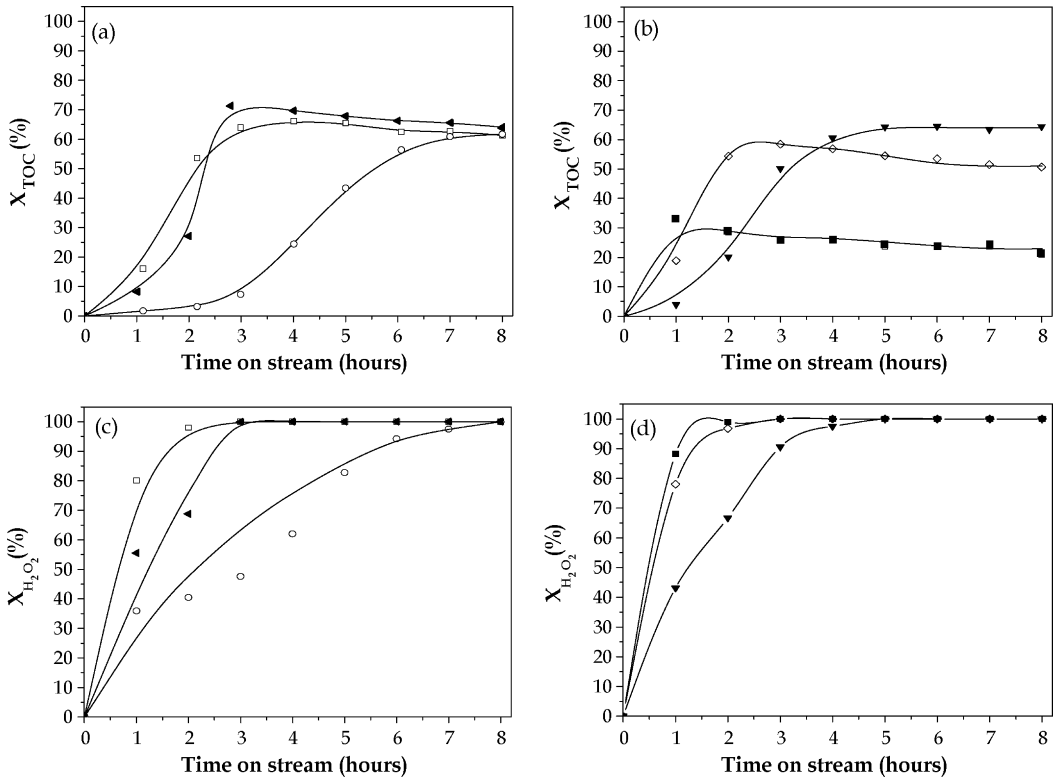


**Fig. 5.** TOC (a and b) and hydrogen peroxide (c and d) conversion profiles for the different iron-containing catalysts prepared by means of direct synthesis and incipient wetness impregnation: (□) $Fe_2O_3$/SBA-15(I), (◀) $Fe_2O_3$/SBA-15(DS), (○) $Fe_2O_3$ + SBA-15(PM), (▼) $Fe_2O_3/SiO_2$(I), (◇) $Fe_2O_3/SiO_2$(DS), and (■) $Fe_2O_3/SiO_2$-PQ(I).

($\eta \approx 0.18$). It must be pointed out that oxygenated by-products (mainly carboxylic acids) formed at high TOC degradation rates are much more refractory than phenolic compounds for its mineralization, which leads to oxidant efficiency values lower than one [24]. The lowest oxidant efficiency of $Fe_2O_3/SiO_2$-PQ(I) could be related to the nature of the commercial silica or the presence of metal traces that enable the decomposition of the oxidant to other less active radical species, different of hydroxyl radicals.

Regarding iron leaching (Fig. 6), it is important to note that catalysts prepared by impregnation ($Fe_2O_3/SiO_2$(I), $Fe_2O_3/SiO_2$-PQ(I) and $Fe_2O_3$/SBA-15(I)) display higher loss of iron in the outlet stream than those prepared by direct synthesis ($Fe_2O_3/SiO_2$(DS) and $Fe_2O_3$/SBA-15(DS)). This fact indicates weaker interactions between the iron species and the silica support for iron-containing catalysts prepared by impregnation, which is not only contributing to a faster catalyst deactivation but also to an additional metal pollution in the treated effluent, as it is the case of $Fe_2O_3$/SBA-15(I) and $Fe_2O_3/SiO_2$-PQ(I) catalysts with iron concentrations in the outlet stream above 100 mg/L. The best stability of $Fe_2O_3/SiO_2$(I), as compared to the other two impregnated catalyst over mesostructured SBA-15 and mesoporous silica-PQ, indicates a stronger interaction between iron particles and silica support. This can be related to the particular physicochemical properties of the silica matrix for supporting small iron clusters. In this sense, the high density of silanol groups that typically provides silica prepared via sol–gel, could be responsible of a stronger interlinking of the impregnated iron species over the silica framework.

Therefore, catalysts prepared by direct synthesis $Fe_2O_3$/SBA-15(DS) and $Fe_2O_3/SiO_2$(DS) as well as impregnated $Fe_2O_3/SiO_2$(I) exhibited a good behaviour with relatively low values, between 10 and 20 mg/L, and slight variation of the iron concentration detected along the time on stream. Profiles of $Fe_2O_3$/SBA-15(I) and $Fe_2O_3/SiO_2$-PQ(I) catalysts, evidence a low durability for long operating times. Moreover, attending to the legal discharge limit for iron concentration (10 mg/L), one of the main aims to apply successfully heterogeneous catalytic systems is the reduction of the iron leaching to lower values, which promote higher durability of the catalyst. In this sense, the physicochemical properties of the materials prepared by direct synthesis, independently of the support used, allow improving the catalytic stability, being consequently more interesting for this kind of applications.

Looking at the pH values, a decrease of the initial phenol aqueous solution pH (ca. 5.5) is observed. This decrease is normally attributed to the formation of carboxylic acids as final refractory by-products of the partial oxidation of phenol as well as protons by Fenton-related reactions [25]. The lowest pH is obtained with the less active catalyst due to more carboxylic acids are formed, which

**Table 3**
Activity and stability of the different iron-containing catalyst under steady-state conditions.

| Catalyst | $X_{TOC}$ (%) | $X_{Phenol}$ (%) | $X_{H_2O_2}$ (%) | $\eta$ | $[Fe]_{leached}$ (mg/L) | pH |
|---|---|---|---|---|---|---|
| $Fe_2O_3$/SBA-15(I) | 61 | 100 | 100 | 0.52 | 123 | 4.0 |
| $Fe_2O_3$/SBA-15(DS) | 64 | 100 | 100 | 0.56 | 14 | 4.3 |
| $Fe_2O_3$ + SBA-15(PM) | 62 | 100 | 100 | 0.53 | 5 | 5.0 |
| $Fe_2O_3/SiO_2$(I) | 64 | 100 | 100 | 0.54 | 20 | 4.2 |
| $Fe_2O_3/SiO_2$(DS) | 52 | 100 | 100 | 0.44 | 11 | 4.0 |
| $Fe_2O_3/SiO_2$-PQ(I) | 21 | 93 | 100 | 0.18 | 120 | 2.3 |

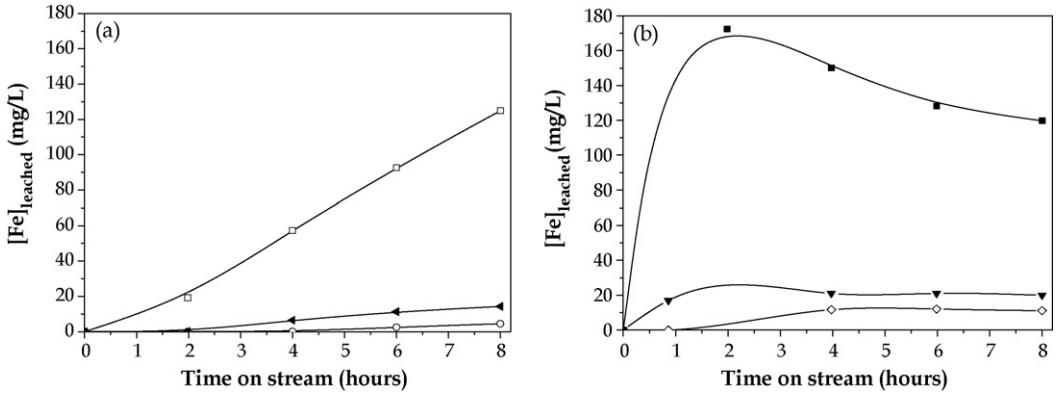


**Fig. 6.** Leached iron concentration for the different iron/silica catalysts prepared by means of direct synthesis and incipient wetness impregnation: (a) (□) $Fe_2O_3$/SBA-15(I), (◄) $Fe_2O_3$/SBA-15(DS), and (○) $Fe_2O_3$ + SBA-15(PM); (b) (▼) $Fe_2O_3/SiO_2$(I), (◇) $Fe_2O_3/SiO_2$(DS), and (■) $Fe_2O_3/SiO_2$-PQ(I).

are not further mineralized by the $Fe_2O_3/SiO_2$-PQ(I) catalytic system, whereas the other catalysts are able to partially mineralize the formed carboxylic acids. Some studies have reported that metal iron leaching of Fenton-like catalysts can be influenced by the solution pH in systems operating in batch conditions [13]. On the contrary, in this study for the continuous treatment of phenol aqueous solution with different catalysts this type of relationship was not evidenced.

Summarizing, catalysts prepared by direct synthesis over mesostructured SBA-15 and mesoporous sol–gel silica showed the best compromise over the catalytic performance, in terms of TOC reduction, and stability, measured as iron leached out from the catalysts to the treated effluent. These materials provide activities above 50% in terms of TOC conversion as well as reduced iron leaching below 15 mg/L. Although the mesostructured $Fe_2O_3$/SBA-15(DS) catalyst presents higher values of TOC degradation (64%) and hydrogen peroxide efficiency, the non-ordered mesoporous $Fe_2O_3/SiO_2$ (DS) prepared via sol–gel is also considered as a potential candidate for its application in industrial catalytic wet peroxide oxidation processes. The decrease of the $Fe_2O_3/SiO_2$(DS) catalytic performance as compared to its counterpart over mesostructured SBA-15 support could be related to its either lower iron content (11.1% versus 14.0%) or lower specific surface area (225 $m^2$/g versus 264 $m^2$/g). Note that the synthesis of $Fe_2O_3/SiO_2$(DS) catalyst is cheaper than that of $Fe_2O_3$/SBA-15(DS) sample since it is not necessarily a highly cost organic molecule template.

## 4. Conclusions

Different iron-containing catalysts based on hematite crystalline iron oxides supported over mesostructured SBA-15 and non-ordered mesoporous silica were tested in an up-flow fixed bed reactor for the continuous catalytic wet peroxide oxidation of phenol aqueous solution. SBA-15 silica support provides iron catalysts with narrower pore size distributions and higher specific surface areas than non-ordered mesoporous silica. The agglomeration process do not produce significant changes in the physicochemical properties of the precursor powder catalysts, although in the case of mesostructured SBA-15 silica supports, a more accentuated reduction of the specific surface was observed.

The activity of the iron-containing catalyst in terms of TOC conversion and oxidant efficiency was mainly affected by the type of silica support, whereas the iron resistance to be leached out was principally dependent on the synthesis method. The iron incorporation in the silica matrix by means of direct synthesis (co-condensation of iron and silica sources) has provided higher stability of the supported iron species. In contrast, those catalysts prepared by incipient wetness impregnation proved higher losses of iron in the treated aqueous solution (up to 100 mg/L). Mesostructured $Fe_2O_3$/SBA-15 is shown as the best catalyst with a high catalytic performance and reduced iron leaching for the treatment of phenolic aqueous solutions. Non-ordered mesoporous $Fe_2O_3/SiO_2$(DS) catalyst prepared via sol–gel in absence of organic template was also considered an interesting candidate for its application in wet peroxide oxidation processes. Both catalysts achieved a total phenol removal with TOC reductions above 50% and relative low iron leaching (below 15 mg/L) operating for 8 h on stream.

## Acknowledgements

The authors thank "Ministerio de Ciencia y Tecnología" for the financial support through the project Consolider-Ingenio 2010 and "Comunidad de Madrid" through the project P-AMB-000395-0505.

## References

[1] J.R. Katzer, H.H. Ficke, A. Sadana, J. Water Pollut. Control Fed. 48 (1976) 920.
[2] W.H. Glaze, J.W. Kang, D.H. Chapin, Ozone Sci. Eng. 9 (1987) 335.
[3] C.A. Tolman, W. Tumas, S.Y.L. Lee, D. Campos, in: D.H.R. Barton (Ed.), The activation of dioxygen and homogeneous catalytic oxidation, Plenum Press, New York, 1993, p. 57.
[4] L. Plant, M. Jeff, Chem. Eng. 16 (1994) 16.
[5] E. Neyens, J. Baeyens, J. Hazard. Mater. 98 (2003) 33.
[6] H.J. Fenton, J. Chem. Soc. 65 (1894) 899.
[7] G. Busca, S. Berardinelli, C. Resini, L. Arrighi, J. Hazard. Mater. 160 (2008) 265.
[8] C.H. Walling, Acc. Chem. Res. 8 (1975) 125.
[9] G. Ovejero, J.L. Sotelo, F. Martínez, J.A. Melero, L. Gordo, Ind. Eng. Chem. Res. 40 (2001) 3921.
[10] J.A. Melero, G. Calleja, F. Martínez, R. Molina, K. Lázár, Micropor. Mesopor. Mater. 74 (2004) 11.
[11] N. Crowther, F. Larachi, Appl. Catal. B: Environ. 46 (2003) 293.
[12] G. Calleja, J.A. Melero, F. Martínez, R. Molina, Water Res. 39 (2005) 1741.
[13] J.A. Melero, G. Calleja, F. Martínez, R. Molina, M.I. Pariente, Chem. Eng. J. 131 (2007) 245.
[14] F. Martínez, M.I. Pariente, J.A. Melero, J.A. Botas, J. Adv. Oxid. Technol. 11 (2008) 75.
[15] M.I. Pariente, F. Martínez, J.A. Melero, J.A. Botas, T. Velegraki, N.P. Xekoukoulotakis, D. Mantzavinos, Appl. Catal. B: Environ. 85 (2008) 24.
[16] E. Guélou, J. Barrault, J. Fournier, J.M. Tatibouët, Appl. Catal. B: Environ. 44 (2003) 1.
[17] S. Perathoner, G. Centi, Top. Catal. 33 (2005) 207.
[18] S. Caudo, G. Centi, Ch. Genovese, S. Perathoner, Appl. Catal. B: Environ. 70 (2007) 437.
[19] F. Martínez, Y.J. Han, G.D. Stucky, J.L. Sotelo, G. Ovejero, J.A. Melero, Stud. Surf. Sci. Catal. 142 (2002) 1109.
[20] M.D. Alcalá, C. Real, Solid State Ionics 177 (2006) 955.
[21] J.R. González-Velasco, M.A. Gutierréz-Ortiz, R. Ferret, A. Aranzabal, J.A. Botas, J. Mater. Sci. 34 (1999) 1999.
[22] F. Martínez, J.A. Melero, J.A. Botas, M.I. Pariente, R. Molina, Ind. Eng. Chem. Res. 46 (2007) 4396.
[23] L. Vradman, M.V. Landau, D. Kantorovich, Y.A. Koltypin, Micropor. Mesopor. Mater. 79 (2005) 307.
[24] G. Centi, S. Perathoner, T. Torre, M.G. Verduna, Catal. Today 55 (2000) 61.
[25] M. Noorjahan, V. Durga Kumari, M. Subrahmanyam, L. Panda, Appl. Catal. B: Environ. 57 (2005) 291.